

In Situ Neutron Diffraction Studies of Methane Hydrate Formation and Decomposition[†]

Piers Buchanan,[‡] Alan K. Soper,[§] Robin E. Westacott,^{||} Jefferson L. Creek,[⊥] and Carolyn A. Koh^{*‡}

Department of Chemistry, King's College London, Strand, London WC2R 2LS, U.K.; ISIS Facility, Rutherford Appleton Laboratory, Chilton, Didcot, Oxon OX11 0QX, U.K.; Chemical Engineering, School of Engineering and Physical Sciences, Heriot-Watt University, Edinburgh EH14 4AS, U.K.; and Chevron Petroleum Technology, Houston, Texas 77082

The hydration structure around methane hydrate during formation and decomposition has been determined using neutron diffraction with isotopic substitution. Measurements were made over a temperature range of 20 °C to 4 °C and at a constant pressure of 14.5 MPa. The first order difference from the neutron diffraction results suggests that there is an interesting two-stage process to methane hydrate formation that is not evident in the decomposition process. Empirical potential structure refinement (EPSR) of this new data, using the appropriate methane/water weightings for each time segment, confirms an earlier finding that methane hydrate formation increases the diameter of the hydration sphere by approximately 1 Å. In addition, the presence of solvent separated methane molecules is confirmed by the estimated C–C pair distribution function separation of 7 Å.

Introduction

Clathrate hydrates are crystalline solids composed of hydrogen-bonded water molecules which are arranged as polyhedral cavities.¹ These water cavities can trap a wide range of guest molecules, including methane, carbon dioxide, and propane. The formation of natural gas hydrates in gas and oil subsea pipelines leads to blockage of these pipelines, which can result in huge economic losses and catastrophic safety consequences to industry.^{1,2} Methane hydrates have also been found to occur naturally in sediments in the deep ocean continental margins and permafrost regions.¹ The vast quantities of methane contained within these natural hydrate deposits offer a clean energy alternative to the conventional energy supplies in current use.

A fundamental understanding of the molecular processes involved during natural gas hydrate formation and decomposition is needed in order to progress with understanding and tackling some of the technological challenges presented by these materials.³ In particular, examining molecular-level details of gas hydrate formation and decomposition can provide insight into the structure of the liquid phase immediately prior to formation or after dissociation of the hydrate crystal lattice.

The "SANDALS" diffractometer (small angle neutron diffractometer for liquid and amorphous samples) at the ISIS facility in the United Kingdom is optimized for the study of systems containing light atoms such as deuterium or hydrogen. In particular, the angles of the detectors ($37^\circ > 2\theta > 3.5^\circ$) are low in order to minimize the correction

for inelastic neutron scattering (see Figure 1). In excess of one thousand detectors allow highly accurate neutron diffraction with isotopic substitution measurements to be made.

Experimental Details

Neutron diffraction measurements have been performed on the SANDALS diffractometer at the ISIS spallation neutron source on the methane/water system over a range of temperatures at a constant pressure of 14.5 MPa. The SANDALS neutron beam dimensions were set to approximately 18 mm by 18 mm. Methane hydrate formation was induced "in situ" by vigorous agitation of the methane/water mixture contained in a cylindrical TiZr high pressure, variable temperature reactor of internal diameter 15 mm. On complete hydrate conversion of the liquid within the neutron beam, the temperature was subsequently increased in stages from 18 °C to 20 °C until the methane hydrate was completely decomposed. At this stage, the temperature was well outside the hydrate formation region and the neutron diffraction pattern gave no indication of Bragg reflections due to hydrate crystals. This process was carried out with both deuterated methane and protiated methane; that is, both CH₄/D₂O and CD₄/D₂O hydrates were made and their respective neutron diffraction patterns measured.

Neutron diffraction data were collected for methane hydrate during both hydrate formation and decomposition stages. Diffraction data for the empty pressure cell, a vanadium rod, and the empty instrument were also collected. The data were analyzed using the new program "GUDRUN", developed at ISIS, which analyzes amorphous time-of-flight neutron diffraction data. This program is a development on the ATLAS suite of programs⁴ in that it analyzes the data in one step and for each individual detector before the final merge. The program corrects for attenuation, multiple scattering, and Placzek effects, generating a total structure factor $F(Q)$ for a given system. This is a weighted sum of the partial structure factors or $S(Q)$'s. For a *binary* system this can be represented using

[†] This contribution will be part of a special print edition containing papers presented at the 9th Asian Pacific Confederation of Chemical Engineering Congress, Christchurch, New Zealand, September 29 to October 3, 2002.

* To whom correspondence should be addressed. E-mail: carolyn.koh@kcl.ac.uk.

[‡] King's College London.

[§] Rutherford Appleton Laboratory.

^{||} Heriot-Watt University.

[⊥] Chevron Petroleum Technology.

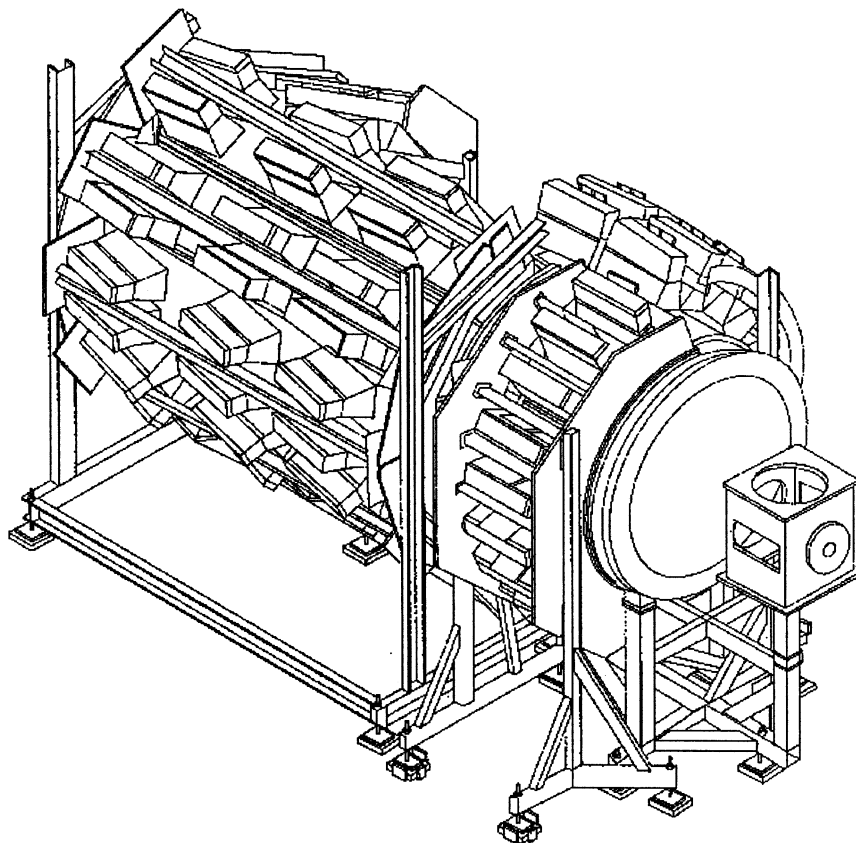


Figure 1. SANDALS diffractometer at the ISIS facility. At the front of the instrument is the sample space. (Reproduced with permission from the SANDALS manual, RALTR 98006, 1998.)

Table 1. Neutron Weighting Factors (NWF) for the 10 Correlations for the Methane/Water System for the Case of Fully Formed Hydrate in Both the Deuteriated and Protiated Cases

	tot neutron diffraction pattern NWF (deut/prot methane)	1st-order difference diffraction pattern NWF (i.e., deut minus prot)
methane–methane correlations	C–C 0.0009/0.0009	
	C–M ^a 0.0072/–0.0040	C–M 0.0112
	M–M 0.0144/0.0045	M–M 0.0099
water–water correlations	O–O 0.0225/0.0225	
	O–H 0.1035/0.1035	
	H–H 0.1190/0.1190	
methane–water correlations	C–O 0.0090/0.0090	
	C–H 0.0206/0.0206	
	M–O 0.0360/–0.0202	M–O 0.0562
	M–H 0.0828/–0.0464	M–H 0.1292

^a M indicates a methyl hydrogen.

the following equation:

$$F(Q) = \sum_{\alpha} \sum_{\beta} c_{\alpha} c_{\beta} b_{\alpha} b_{\beta} (S_{\alpha\beta}(Q) - 1) \quad (1)$$

where c is the concentration of the atomic species α and β and b represents their neutron scattering lengths. The coefficients multiplying the partial structure factor, $c_{\alpha} c_{\beta} b_{\alpha} b_{\beta}$, are the so-called neutron weightings and can be found in Table 1 of this paper.

The sine Fourier transform of $F(Q)$, called $G(r)$ or the total radial distribution function, is calculated using the following equation. This gives the probability that any atom in a given system will be at a distance r given that there

is an atom of any type at the origin.

$$G(r) = \frac{1}{2\pi^2 \rho r} \int F(Q) Q \sin(Qr) dQ \quad (2)$$

This total radial distribution function can be broken down into a weighted sum of all the partial pair distribution functions, $g_{\alpha\beta}(r)$. ($g_{\alpha\beta}(r)$ is defined as being the relative density of atoms of type β at a distance r from an atom of type α at the origin. Thus, $g_{\alpha\beta}(r) \rightarrow 1$ as $r \rightarrow \infty$.)

$$G(r) = \sum_{\alpha} \sum_{\beta} c_{\alpha} c_{\beta} b_{\alpha} b_{\beta} (g_{\alpha\beta}(r) - 1) \quad (3)$$

Table 1 illustrates that there are 10 partial structure factors that make up the total structure factor, $F(Q)$ of the methane/hydrate system. It can be seen in the example given for fully formed methane hydrate (i.e. 1 methane molecule/5.75 water molecules) that, by subtracting the $F(Q)$ of $\text{CD}_4 \cdot 5.75\text{D}_2\text{O}$ from the $F(Q)$ for $\text{CH}_4 \cdot 5.75\text{D}_2\text{O}$, the first-order difference is dominated by the M–O and M–H correlations (where M represents the hydrogen on the methane molecule).

Further molecular-level details during the hydrate formation and decomposition processes were extracted from the neutron data using the empirical potential structure refinement (EPSR) method developed by Soper.⁵ This technique allows a basic interatomic potential (the reference potential) to be refined given the neutron diffraction data and a starting structure. In the case of this paper, the starting interatomic potential for methane was a simple Lennard-Jones model and the water potential was the SPC/E potential.⁶ The starting structure was a box containing the appropriate number of methane and water molecules, randomly located and orientated. Initially the

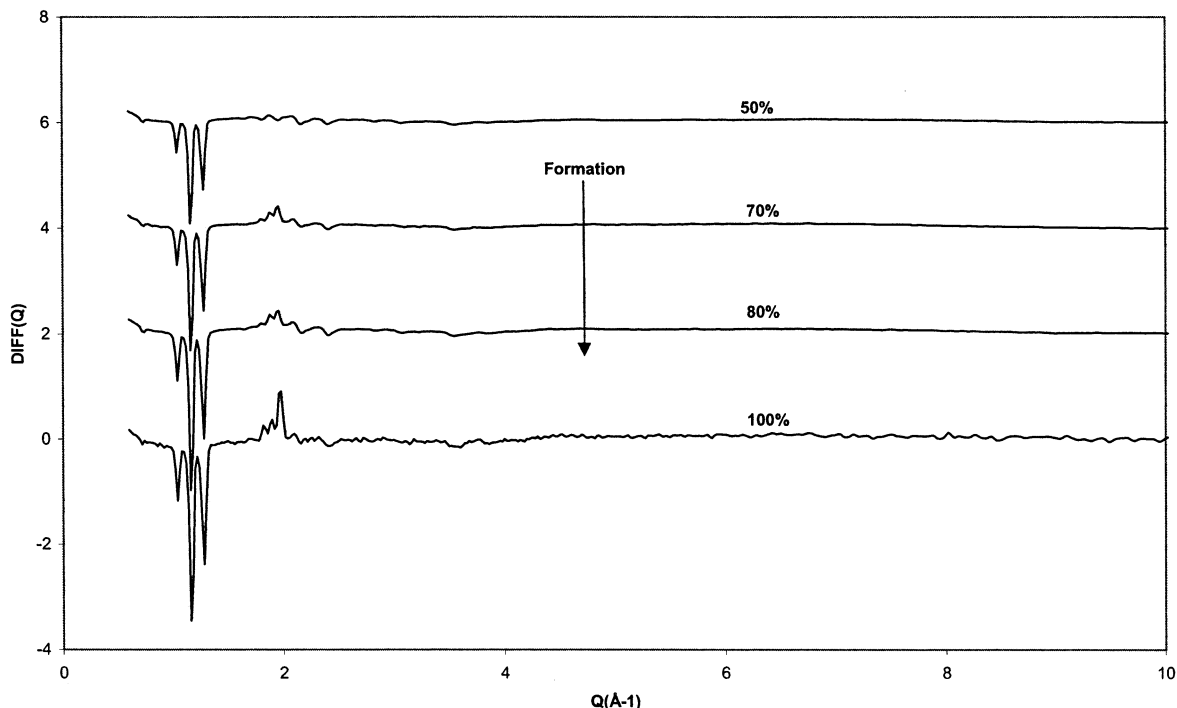


Figure 2. Neutron diffraction first-order difference measurements for the formation of methane hydrate ranging through the following percentages of hydrate formed: 50%, 70%, 80%, and 100%. Each difference function is displaced on the y axis by 2 in relation to the previous one. The arrow shows the direction of formation.

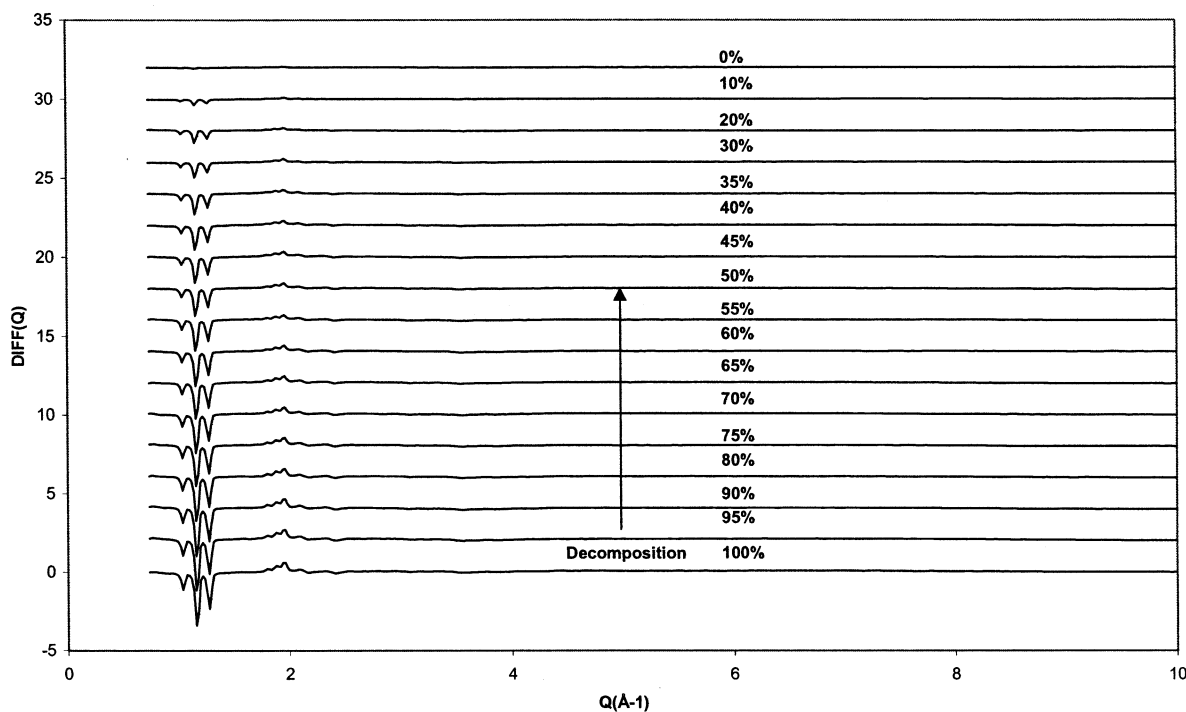


Figure 3. Neutron diffraction first-order difference measurements for the decomposition of methane hydrate ranging through the following percentages of hydrate formed: 0%, 10%, 20%, 30%, 35%, 40%, 45%, 50%, 55%, 60%, 65%, 70%, 75%, 80%, 90%, 95%, and 100%. Each difference function is displaced on the y axis by 2 in relation to the previous one. The arrow shows the direction of decomposition.

reference potential was used without refinement and the structure was refined using the neutron diffraction data. Subsequently, the reference potential was perturbed so that the experimental data were matched as closely as possible by the simulated neutron diffraction pattern. Two simulations were carried out—one for the case of fully formed methane hydrate and one for the case where methane hydrate had been half formed. The EPSR simulation for

fully formed hydrate had 200 methane molecules and 1150 water molecules for its model whereas the half formed hydrate EPSR simulation had 100 methane molecules and 1150 water molecules. This is the appropriate proportion of molecules, given their respective stoichiometries.

Results and Discussion

Figure 2 shows the neutron diffraction first-order difference measurements ($\text{CD}_4 \cdot \text{D}_2\text{O} - \text{CH}_4 \cdot \text{D}_2\text{O}$) for the

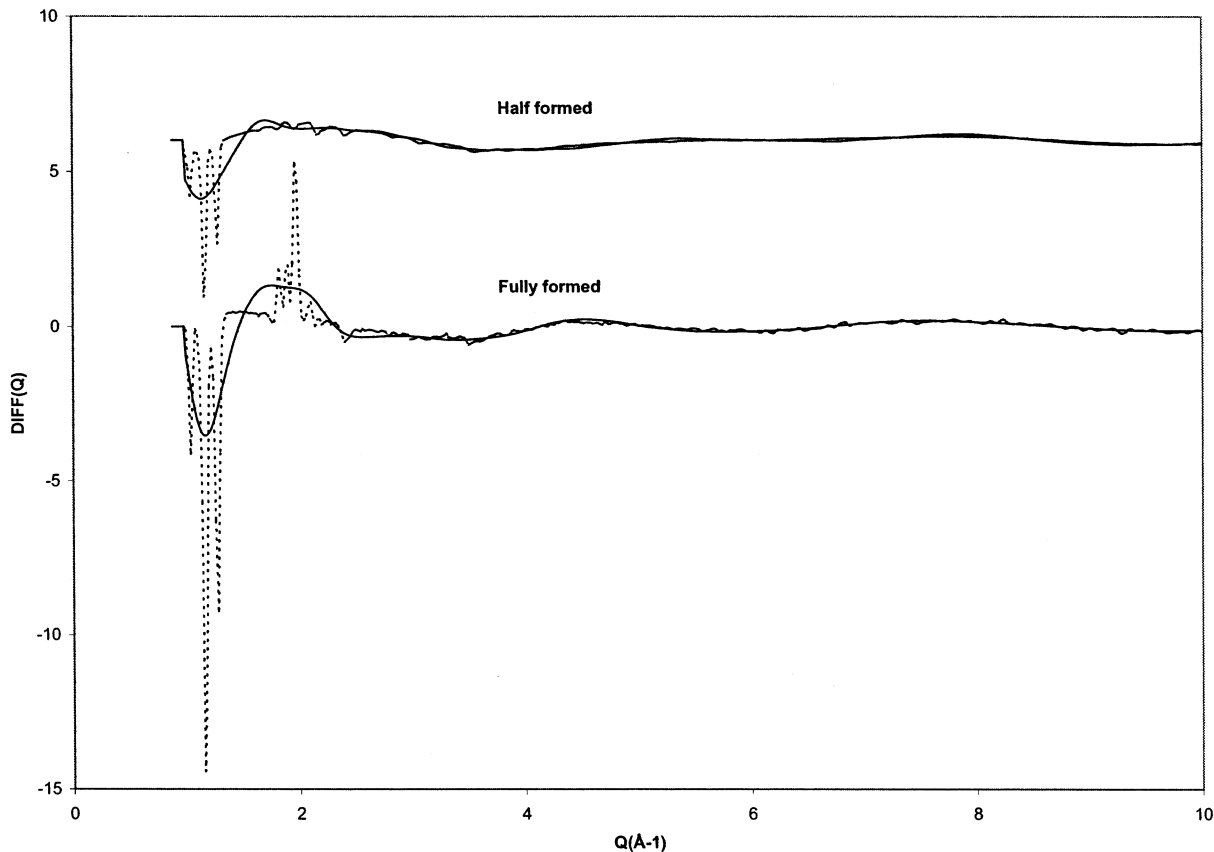


Figure 4. Difference functions for half formed (displaced by 6 on the y axis) and fully formed (undisplaced) methane hydrate. The experimental data are indicated by dashed lines, and the EPSR fits are indicated by unbroken lines.

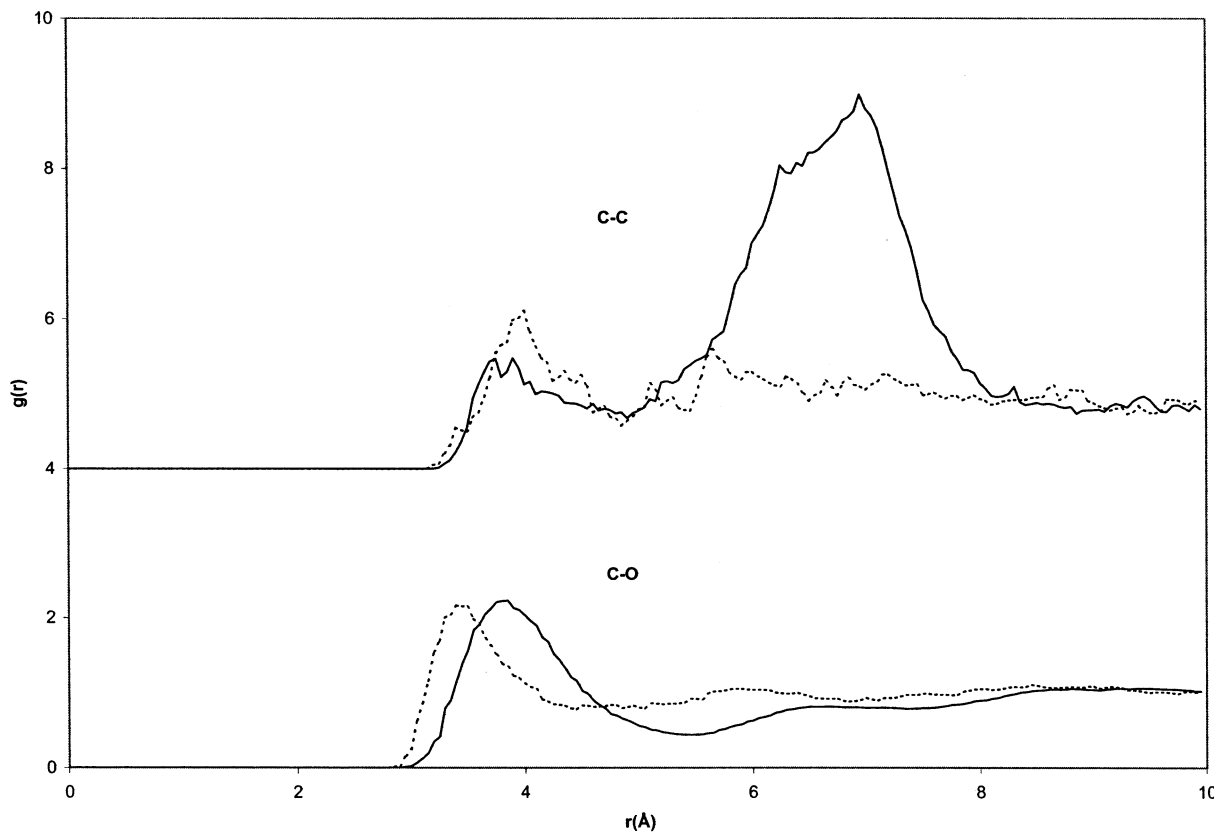


Figure 5. Estimated radial distribution functions for the C-C (displaced by 4 on the y axis) and C-O (undisplaced) correlations for both the half formed (dashed lines) and fully formed (unbroken lines) methane hydrate.

formation stages of methane hydrate (50%, 70%, 80%, and 100% hydrate formation). Figure 3 shows the equivalent

first-order difference functions for the decomposition phase (100% to 0% hydrate formation). It is notable that at 50%

hydrate formation the down-peaks in the 1 \AA^{-1} region are present in both the growth and decomposition phases. However, the difference between the first-order differences for the 50% formed case during the formation and decomposition processes is that the up-peaks in the 2 \AA^{-1} region are only present in the decomposition phase. Examining Figure 2 suggests that there are two stages to the formation process in which the down-peaks are established early on in the formation process and then the up-peaks in the 2 \AA^{-1} region become evident later. Conversely, Figure 3 reveals a smooth transition in the first-order difference from fully formed hydrate to methane gas dissolved in water. A potential reason behind this two-step formation process would be long range ordering occurring first in the methyl hydrogen–water hydrogen and methyl hydrogen–water oxygen correlations in the initial phase of methane hydrate formation followed by a more local ordering of the methane molecules.

Figure 4 illustrates the EPSR fits to the neutron diffraction first-order difference data for half and fully formed methane hydrate. Because of limitations in the size of the simulation box, the Bragg peaks cannot be reproduced by the simulation but the diffuse scattering has been fitted successfully. Figure 5 shows the estimated C–C and C–O pair distribution functions generated from the two EPSR simulations. The C–C pair distribution function in the case of both half and fully formed hydrate shows evidence of direct contact (around 4 \AA) between methane molecules. However, in the case of fully formed hydrate there is considerable evidence of solvent separated pairs in the broad peak at around 7 \AA . This C–C distance is consistent with the crystal structure of methane hydrate.¹ The first peak in the C–O pair distribution function has increased in distance by approximately 0.5 \AA in the fully formed hydrate compared to the half formed hydrate. This confirmed earlier findings⁷ that the hydration sphere of water around methane expands by 1 \AA after formation. The first C–O coordination number (indicating the number of water molecules in the hydration sphere around a carbon atom) has increased from 16 ± 1 for half formed to 20 ± 1 for fully formed hydrate. This value of 20 ± 1 is still slightly lower than the expected value of 23 for type I hydrate

obtained from the crystal structure; however, this is not unreasonable given that the model used for the EPSR simulation was a disordered rather than crystalline model.

Conclusion

The local structure of water around methane has been investigated using neutron diffraction with isotopic substitution. These measurements have demonstrated that both the formation and decomposition processes of methane hydrate can be successfully tracked as a function of time using neutron diffraction with isotopic substitution. A major achievement in these experiments was the ability to exactly match the $\text{CH}_4/\text{D}_2\text{O}$ experiment with the $\text{CD}_4/\text{D}_2\text{O}$ experiment, with excellent control of the hydrate formation and decomposition processes. The previous finding⁷ that the methane hydration shell expands when hydrate is formed has been confirmed.

Acknowledgment

The authors also thank Katan Hirachand and Minjas Zugik for their help with the experimental measurements. The technical support of John Dreyer, Rob Done, and Robin Humphreys at ISIS is gratefully acknowledged.

Literature Cited

- (1) Sloan, E. D. *Clathrate Hydrates of Natural Gases*, 2nd ed.; Marcel Dekker: New York, 1997.
- (2) Englezos, P. *Ind. Eng. Chem. Res.* **1993**, *32*, 1251–1274.
- (3) Koh, C. A. *Chem. Soc. Rev.* **2002**, *31*, 157–167.
- (4) Soper, A. K.; Howells, W. S.; Hannon, A. C. *ATLAS: Analysis of Time-of-Flight Data from Liquid and Amorphous Samples*, Version 1.0; Rutherford Appleton Laboratory Report RAL-89-046; 1989.
- (5) Soper, A. K. *Chem. Phys.* **1996**, *202*, 295–306.
- (6) Berendsen, H. J. C.; Grigera, J. R.; Straatsma, T. P. *J. Phys. Chem.* **1987**, *91*, 6269.
- (7) Koh, C. A.; Wisbey, R. P.; Wu, X.; Westacott, R. E.; Soper, A. K. *J. Chem. Phys.* **2000**, *113*, 6390–6397.

Received for review September 27, 2002. Accepted January 14, 2003. The authors acknowledge the support of Chevron Texaco, Houston, TX, the EPSRC (GR/R42788/01), NATO (PST.CLG.977-638), and the Gas Research Institute, Chicago, IL.

JE025622+